

YIELD ANALYSIS OF RESIDUES FROM $^{12}\text{C}+^{93}\text{Nb}$ REACTION: PRODUCTION OF MEDICALLY IMPORTANT ^{101m}Rh VIA $^{101}\text{Pd}^*$

MALVIKA SAGWAL, MOUMITA MAITI[†]

Department of Physics, Indian Institute of Technology Roorkee
Roorkee-247667, Uttarakhand, India

*Received 3 November 2022, accepted 7 November 2022,
published online 22 March 2023*

Production of ^{101m}Rh radionuclide, which is a preferred candidate for diagnostic imaging and radiotherapy, has been reported from a heavy-ion reaction $^{12}\text{C}+^{93}\text{Nb}$. In addition to its formation as an evaporation residue of $^{105}\text{Ag}^*$ compound nucleus, it was formed significantly through electron capture decay of its precursor ^{101}Pd within the 39.5–75.9 MeV range. Followed by activation, γ -ray spectroscopy was employed to identify evaporation residues. A maximum yield of 793.4 and 89.4 MBq/C at 71.0 MeV was measured for ^{101}Pd and ^{101m}Rh , respectively, along with other co-produced radionuclides. The conditions for optimizing the yield of ^{101m}Rh to ensure its purity have been discussed. Subsequently, the thick target yield for ^{101m}Rh is estimated using the model code EMPIRE-3.2.2.

DOI:10.5506/APhysPolBSupp.16.4-A39

1. Introduction

Platinum group (Pt, Pd, Rh, Ru, *etc.*) coordination compounds are well-established chemotherapeutic agents [1] due to their chemical reactivity with biological macromolecules. Among them, a large number of Rh complexes, such as [Rh(I) COD bipy]⁺Cl⁻, Rh(II) Carboxylate, Rh(II) Citrate, *etc.*, act against cancers, including, but not limited to Ehrlich ascites carcinoma, L1210 Leukemia, and Lewis lung carcinoma [2–5]. Specific Rh-labeled radiopharmaceuticals are used for tracking their delivery and tumor localization in the body. For instance, ^{101m}Rh (4.34 d), which is nearly optimal for *in vivo* applications such as diagnostic imaging, decays into stable daughter nucleus ^{101}Ru through electron capture (ϵ) by emitting low-energy 306.9 keV γ -ray (81% intense). Additionally, the emission of Auger and Coster–Kronig electrons following ϵ -decay makes it effective in targeted radiotherapy.

* Presented at the Zakopane Conference on Nuclear Physics, *Extremes of the Nuclear Landscape*, Zakopane, Poland, 28 August–4 September, 2022.

[†] Corresponding author: moumita.maiti@ph.iitr.ac.in

^{101}Pd (8.47 h), a natural precursor of ^{101m}Rh , decays through ϵ (100%), and both radionuclides desirably possess a measurable difference in half-lives ($T_{1/2}$). Production routes for both the radionuclides, for which charged particle bombardment through accelerators is recommended, are being investigated. It is due to the feasibility of separating a radionuclide by physical or chemical means to achieve high specific activity [6]. A variety of cyclotron production routes by light-ion-induced reactions have been attempted over the past decades. In the late 70s, Scholz *et al.* [7] and subsequently Lagunas-Solar *et al.* [8, 9] probed the production of ^{101}Pd from proton-induced reactions, *i.e.*, $^{103}\text{Rh}(p, 3n)^{101}\text{Pd}$ and $^{\text{nat}}\text{Pd}(p, 3n)^{101}\text{Ag} \rightarrow ^{101}\text{Pd}$, followed by chemical separation. The proton, deuteron, and helion-induced reaction on $^{\text{nat}}\text{Pd}$, $^{\text{nat}}\text{Ag}$, ^{103}Rh , and $^{101,102}\text{Ru}$, also resulted in ^{101}Pd and ^{101m}Rh (cumulative) in different energy ranges [10–13]. The activation cross section and yield data reported in the literature have added notable worth to such investigations [14].

Some heavy-ion reactions have shown potential as alternate production routes to a good quantity of radionuclides for various pilot studies [15]. However, application-based radionuclide production is scarce through heavy-ion-induced reactions. We experimented to study the reaction mechanism of $^{12}\text{C}+^{93}\text{Nb}$ [16] within the 39.5–75.9 MeV range. The observation of significant production of ^{101}Pd has led us to maneuver the effort towards estimating ^{101}Pd and ^{101m}Rh yields. The main focus of the work revolves around enhancing the isotopic purity of ^{101m}Rh .

2. Experiment and data analysis

The experiment was conducted at the 14 UD BARC-TIFR Pelletron facility in Mumbai, India. The thin ^{93}Nb target and ^{27}Al catcher-foils with thicknesses of 1.3–3.0 and 1.5–1.8 mg/cm², respectively, were placed alternately to make stack-foil assemblies. The ^{12}C beam was used to irradiate the stacked foils, and the details are enlisted in Table 1. Data over a wide range, 39.5–75.9 MeV (lab frame) above the Coulomb barrier (37.7 MeV), were obtained through energy degradation.

Post activation, the offline counting of the induced radioactivity in the target-catcher foils was carried out for a sufficiently long duration intermittently for several days using precalibrated high-purity germanium (HPGe) detector whose energy resolution was 2 keV for a 1332 keV γ -ray peak. The characteristic γ -ray spectra were acquired through the GENIE-2k software for each target-catcher foil to identify the unstable evaporation residues (ERs) produced. The ERs, *viz.*, $^{103,102,101}\text{Ag}$, $^{101,100}\text{Pd}$, $^{101m,100,99m,97}\text{Rh}$, ^{97}Ru , $^{96,95,94}\text{Tc}$, and ^{93m}Mo , were further confirmed through their time-evolved activity profiles. The spectroscopic data and typical γ -ray spectrum can be found elsewhere [16]. Possible uncertainties, including target thickness, area

count statistics, geometry-dependent detector efficiency, and beam current fluctuations have been duly considered during the error estimation in the measured yield.

Table 1. Irradiation details with the ^{12}C beam.

Lab energy [MeV]	Charge state	Irradiation time [h]	Integral charge [μC]	Beam flux [particles/s]
77	6^+	2.3	301.7	3.80×10^{10}
73.5	6^+	3.85	907.1	6.82×10^{10}
63	5^+	2.6	618.0	8.25×10^{10}
50	5^+	3.05	833.1	9.48×10^{10}

3. Results and discussion

The populated ERs having $T_{1/2}$ within several minutes to days have been identified within the 39.5–75.9 MeV range. The measured production cross sections of the populated ERs have been compared with the predictions of EMPIRE-3.2.2 model code [17] to understand the reaction mechanism. The excitation functions of most ERs have been satisfactorily reproduced by EMPIRE with EGSM level density, and hence, the reaction is governed by a combination of the compound and pre-compound mechanisms [16].

Figure 1 (a) depicts through EMPIRE calculations that ^{101}Pd (8.47 h) is the most probable reaction product among others. It is formed by $p3n$ evaporation from the $^{105}\text{Ag}^*$ compound nucleus. Meanwhile, ^{101m}Rh (4.34 d) has nearly one-third of its maximum cross section. The potential of ^{101}Pd as a precursor to enhance daughter ^{101m}Rh activity through ϵ -decay (100%)

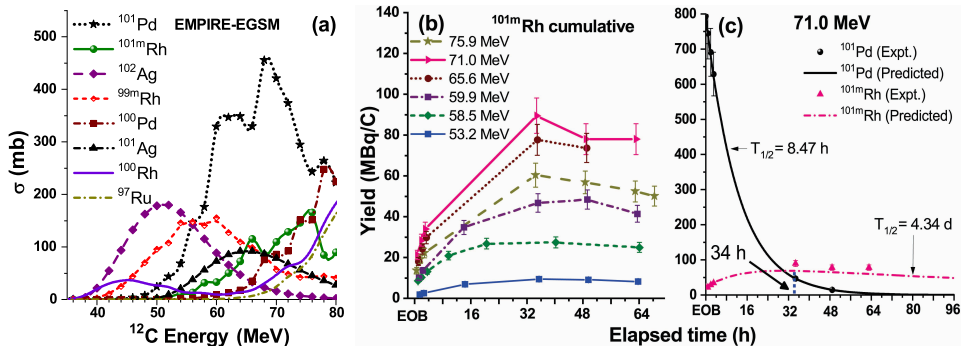


Fig. 1. (a) EMPIRE predicted cross sections of major ERs populated from the $^{12}\text{C}+^{93}\text{Nb}$ reaction. (b) Measured time evolved yield of ^{101m}Rh due to the decay of ^{101}Pd . (c) Successive disintegration profiles of ^{101}Pd and ^{101m}Rh .

is quite evident. In fact, the former is also formed cumulatively from its precursor ^{101}Ag (11.1 min), which gives $^{101}\text{Ag} \rightarrow ^{101}\text{Pd} \rightarrow ^{101m}\text{Rh}$. However, the contribution of ^{101}Ag in ^{101}Pd is rather small [16].

As the radionuclides keep on decaying within the target matrix, we have obtained their decay rates per unit integral charge of the beam to find the normalized radioactivity or yield as a function of elapsed time. For a radionuclide “r”, the yield (Y^r) has been estimated using Eq. (1) where t_w is the waiting or elapsed time, *i.e.*, the time difference between the end of bombardment (EOB) and the start of γ -ray acquisition. C denotes the count rate (/s), ε_γ and I_γ^r are the geometry-dependent detection efficiency of the HPGe and branching intensity of the characteristic γ -ray of the radionuclide, respectively. Z is the charge state of the beam, and I_c is the integral charge in μC collected by the Faraday cup during irradiation

$$Y^r(t_w) = \frac{C Z}{\varepsilon_\gamma I_\gamma^r I_c} \text{ MBq/C} . \quad (1)$$

The directly measured yields of ^{101m}Rh at different energies have been plotted in Fig. 1 (b). The measured EOB yield of ^{101}Pd is 793.4 MBq, and with the lapse of nearly four half-lives (≈ 34 h), around 94% of ^{101}Pd nuclei formed at the EOB decay and the ^{101m}Rh in-growth maximizes. The peak production of cumulative ^{101m}Rh was observed at 71.0 MeV, where its yield reached 21.3 to 89.4 MBq/C. The same has been emphasized in Fig. 1 (c) through the successive disintegration profiles for both the radionuclides.

As our goal is to discuss the ^{101m}Rh production for clinical purposes, it becomes customary to understand its radioisotopic purity. The fate of co-produced radionuclides, excluding other Rh isotopes, at 71.0 MeV has been shown in Fig. 2 (a). The measurement at $t_w = 34.7$ h represented the significant decay of short-lived activities and reduced exposure to personnel.

Subsequently, to ensure the no-carrier-added (NCA) production of ^{101m}Rh , the key task is to eliminate the isotopes of Rh as they can interfere during chemical separation from the target matrix. It can be seen that the yield of ^{99m}Rh (4.7 h) and ^{97}Rh (30.7 min), vanishes with time (Fig. 2 (b)), and only ^{100}Rh contamination contributes up to some extent. The EMPIRE predicted that ^{103m}Rh (56.114 min), ^{102m}Rh (3.742 y), and ^{98}Rh (8.72 min) have not been observed either due to their tiny production cross section or short half-life with a moderate production that subsides quickly due to ϵ -decay. Hence, after the waiting period of ≈ 34 h, minimal isotopic impurity in ^{101m}Rh is ensured. A suitable chemical separation procedure for ^{101m}Rh can be started post 32–34 h of EOB.

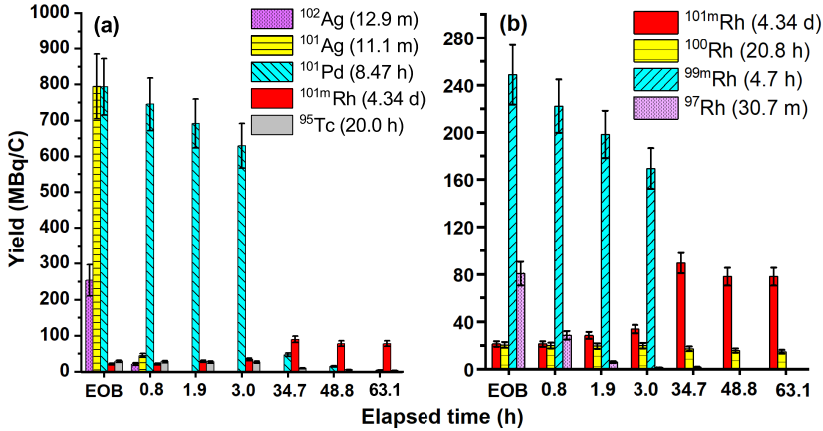


Fig. 2. Time-evolved yields of populated radionuclides from the $^{12}\text{C}+^{93}\text{Nb}$ reaction at 71.0 MeV (a) excluding other Rh isotopes, and (b) only for the Rh isotopes.

The thick target yield (TTY) estimation is valuable as it depicts the reaction's feasibility for producing the application-oriented radionuclide. The EMPIRE estimation over a wide energy range finds that the energy interval of 39–77 is suitable for the maximum and nearly contamination-free production of ^{101m}Rh (Fig. 1 (a)). As the model code is justifying our data quite well [16], we have theoretically achieved 106 MBq/C of the TTY for ^{101m}Rh (cumulative) for a 28 mg/cm² thick ^{93}Nb target at the EOB within the 39–77 MeV energy window.

4. Conclusion

This work details the yield estimation of ^{101m}Rh and its precursor ^{101}Pd from the $^{12}\text{C}+^{93}\text{Nb}$ reaction within the 39.5–75.9 MeV range. The excitation function study reveals that ^{101}Pd has a significant cross section among all the observed radionuclides and can be an alternative route to produce ^{101m}Rh . The EOB experimental yield comparison of all the radionuclides has been made where the maximum measured yield of ^{101m}Rh and ^{101}Pd is 89.4 MBq/C and 793.4 MBq/C, respectively, at 71.0 MeV. The waiting time of ≈ 34 h is required to optimize the in-growth of ^{101m}Rh in the target matrix and minimize the isotopic contaminants to ensure the chemical purity of ^{101m}Rh . The calculated thick target yield for cumulative ^{101m}Rh is 106 MBq/C for a 28 mg/cm² thick target of ^{93}Nb in the 39–77 MeV range. The laboratory-scale reaction further envisages the production of ^{101m}Rh on an industrial scale with a high-beam current followed by an appropriate chemical separation procedure.

The authors thank the BARC-TIFR Pelletron staff for their support during the experiment. Close cooperation from TISISPEC laboratory colleagues from IIT Roorkee is highly appreciated. The Research Grant No. 03(1467)/19/EMR-II from CSIR(IN) and Research Fellowship from the MHRD, Government of India, is gratefully acknowledged.

REFERENCES

- [1] M.J. Cleare, *Coord. Chem. Rev.* **12**, 349 (1974).
- [2] T. Giraldi *et al.*, *Chem.-Biol. Interact.* **9**, 389 (1974).
- [3] A. Erck *et al.*, *Proc. Soc. Exp. Biol. Med.* **145**, 1278 (1974).
- [4] S. Zyngier *et al.*, *Braz. J. Med. Biol. Res.* **22**, 397 (1989).
- [5] M.L.B. Carneiro *et al.*, *J. Nanobiotechnol.* **9**, 11 (2011).
- [6] I.A.E.A., Technical Report Series No. 468, 2009.
- [7] K.L. Scholz *et al.*, *Int. J. Appl. Radiat. Isot.* **28**, 207 (1977).
- [8] M.C. Lagunas-Solar *et al.*, *J. Radioanal. Chem.* **68**, 245 (1982).
- [9] M.C. Lagunas-Solar *et al.*, *Int. J. Appl. Radiat. Isot.* **35**, 743 (1984).
- [10] M.U. Khandaker *et al.*, *Nucl. Instrum. Methods Phys. Res. B* **268**, 2303 (2010).
- [11] M.S. Uddin *et al.*, *Appl. Radiat. Isot.* **62**, 533 (2005).
- [12] F. Ditrói *et al.*, *Nucl. Instrum. Methods Phys. Res. B* **269**, 1963 (2011).
- [13] Y. Skakun *et al.*, *Appl. Radiat. Isot.* **66**, 653 (2008).
- [14] M. Maiti, *J. Radioanal. Nucl. Chem.* **297**, 319 (2013).
- [15] D. Kumar *et al.*, *J. Radioanal. Nucl. Chem.* **313**, 655 (2017).
- [16] M. Sagwal *et al.*, *Eur. Phys J. Plus* **136**, 1057 (2021).
- [17] M. Herman *et al.*, *Nucl. Data Sheets* **108**, 2655 (2007).